CHARACTERIZING FIRST, SECOND, AND THIRD-ORDER WRINKLE RIDGES ON THE MOON. N. R. Gonzales[1], J. D. Clark[1], M. S. Robinson[1], T. R. Watters[2], T. Frueh[3], [1]School of Earth and Space Exploration, Arizona State University, Tempe, AZ 85287 (ngonzales@ser.asu.edu), [2]Center for Earth and Planetary Studies, National Air and Space Museum, Smithsonian Institution, Washington, DC, [3]Institut für Planetologie, Westfälische Wilhelms-Universität Münster, Wilhelm-Klemm-Str.10, 48149 Münster, Germany.

Background: The evolution of stresses acting on rocky bodies is recorded by the variety and type of tectonic landforms found in its crust. Over time, the dense basalt layers that fill basins like Mare begin to subside, creating features we call wrinkle ridges (WRs). WRs can be 10's of km tall and well-defined, a few m tall and wide and hard to see, inter-braided, and even concentric to their host basin, each of which contributes to one overarching question: what do the different geomorphic expressions of a WR tell us about their formation histories? Herein, we will expand on criteria from [1] to more clearly distinguishing the three main geomorphic expressions of a WR (first, second, and third-order ridges) to interpret their origin. Although the criteria presented in this abstract were developed for the Moon, these criteria can also be applied to WRs on other rocky bodies.

WRs are positive relief products of contractional tectonics, most commonly described as a pair of sinuous anticlines: a narrow, segmented ridge superimposed atop a broad, gently-sloped arch [1-7], both of which are commonly asymmetric with one significantly steeper slope [1-2,7-9]. The asymmetry of the slopes is often attributed to the presence of both a fault and a fold. However, the presence of both arch and ridge implies a listric fault geometry [1,10] rather than a fault-bend fold or fault-propagation fold as had previously been considered by [7]. Most WRs share enough morphology with thrust faults on Earth that they are often described as ~30°, shallowly rooted thrust faults [1]. Since we do not have a technique to map the subsurface structure on the Moon, the angle and shape (planar or listric) of the fault are still being debated [1].

WRs are similar to lobate scarps, as both are thrust faults, but WRs are generally thought to run deeper and are the result of subsidence from loading in basalt-filled basins [1,11-12]. On the Moon, WRs are associated with mare-filled basins [1], which in turn adds a bias: they are mostly found on the nearside [1,11]. To date, the modeling of lunar WRs has focused on those in mascon basins [1], which are basins with anomalous "mass concentrations" creating a positive free-air gravity anomaly at the basin center surrounded by a negative gravity anomaly ring at the basin margin [13-16].

The State of the Art: WRs exhibit a maximum width of 20 km, length of 300 km, and height of 0.5 km [1,5]. However, these dimensions describe the entirety of a WR and do not address the complexities of the branching fault structure, which gives WRs a braided appearance (Figs. 1-2).

Two factors have traditionally been used to determine which inter-braided WR feature is a first, second, or third-order ridge: *1) scale of relief, width, and length* [2], and *2) orientation of the ridge* [1,5]. Both of factors should be considered *with respect to the arch it is superposed on top of*, and consider *whether both arch and ridge are present:*

(1) Scale: There are 3 accepted orders of ridges, differentiated by orders of magnitude of scale [2,11]. First-order, or primary ridges, are the largest, on the order of 100's meters tall and 10's km wide (Figs. 1-2), while second and third-order ridges are one and two orders of magnitude smaller, respectively [1-2] (Table 1). These smaller ridges are thought to be either contractional strain accommodation features resulting from shallow, branching faults, or buckling of the upper layers of Mare basalts [2,17] (Fig. 1).

(2) Location with Respect to Arch: Primary ridges are typically parallel to the arch. Secondary and tertiary are often described as flanking the primary ridge and arch or capping the primary ridge [1-2,5,7].

What Next? Terminology is key here. Primary, secondary, and tertiary imply that the primary came first, but this may not be the case. Recent work examining the possibility of recent activity on small wrinkle ridges [18] expanded upon a previous global WR map [9] and included additional, small-scale, stand-alone WR [18]. Because the first-order ridges account for the majority of the shortening within a basin, it is possible that global strain modeling, which focuses only on the contributions of first-order ridges, underestimates the actual strain. While some inter-braiding of a WR may be a result of fault branching (Fig. 1), this is not always the explanation for different scales of a wrinkle ridge [19]. Primary and secondary are not a proxy for WR age nor formation chronology.

Basin morphology also plays a role in the scale and formation of a WR. The thickness and lamination properties of basalt layers within a basin likely play an important role in determining the scale and formation history of a WR [1]. Some WRs are considered to be deeply rooted (20+ km [1,20]) due to their large elevation offsets (when comparing the basin interior and exterior slopes of the WR) from which they derive their name: elevation offset, or EO ridge [1,19-20]. These EOs are exclusive to mascon basins and are thought to be controlled by reactivated normal faults from the basin's formation [1]; as such they likely have a different formation history than other wrinkle ridges which are the result of basin loading after formation.

In order to update the strain estimates per lunar basin, we will need to establish whether each individual WR is part of a braided formation, or if it stands alone. The next step for this work is to categorize each individual WR basin by basin to further examine trends and formation histories of WR.

Feature		Width	Height	Length	Location (with respect to arch)
Type	Order				
Arch	N/A	*1s - 10s km*	*10s m*	< 300 km	N/A
ridge	first	*1s km*	*10s - 100s m*	10s - 100s km	parallel to arch
	second	*100s m*	*10s m*	1s - 10s km	cap/flank
	third	*10s m*	*1s m*	1s - 10s km	cap/flank

Table 1. *Scale and ridge location with respect to the arch. Relief and width of the ridge and arch are derived from [2] establishing the orders of magnitude of each ridge to account for variability in measurement techniques, and now with two additional columns describing the length of the ridge (as an approximate scale), and orientation relative to the arch and primary ridge. Max arch length from [1,5].*

References: [1] Watters, T. R. (2022). JGR: Planets, 127, e2021JE007058. https://doi.org/10.1029/2021JE007058 [2] Watters, T. R. (1988). JGR vol 93, no. B9. [3] Strom, R. G. (1972) The Moon, p 187-215. [4] Bryan, W. B., and M. L. Adams (1973) Apollo 17 Preliminary Science Report. NASA SP-330. [5] Sharpton, V. L., and J. W. Head (1988) Proceedings of the 18th LPSC. [6] Plescia, J. B., and Golombek, M. P. (1985) LPSC XI Abs#1340. [7] Plescia, J. B., and Golombek, M. P. (1986) GSA Bulletin v. 97 [8] O. Karagoz, M. E. Aksoy, G. Erkeling (2018) EPSC2018-1009-1, vol 12. [9] Thompson et al. (2017), LPSC XLVIII Abs#2665 [10] Watters, T. R. (2004) Icarus171 p. 284-294. [11] Watters, T. R. and Schultz, R. A. (2010) Planetary Tectonics, Cambridge Univ. Press. https://doi.org/10.1017/CBO9780511691645 [12] Clark et al. (2017) LPSC XLVIII Abs# 1001 [13] Lemoine, et al. (2014) Geophysical Research Letters v. 41, iss. 10. [14] Melosh, H. J., et al. (2013) Science Mag v 340. [15] Solomon, S. C., and Head, J. W. (1979) JGR v. 84, no. B4. [16] Solomon, S. C., and Head, J. W. (1980) Reviews of Geophys. and Space Phys., v. 18, no. 1, p 107-141. [17] Watters (1991) JGR v. 96, no. E1 [18] Nypaver, Cole; Thomson, Bradley J. (2022): https://doi.org/10.1029/2022GL098975 figshare. Dataset. https://doi.org/10.6084/m9.figshare.19491668.v3 [19] Schultz, R., (2000) JGR. v. 105 no. E5. [20] Byrne, P. K., et al. (2015) Earth and Planetary Sci Letters 427 183-190. [21] Golombek, M. P., Plescia, J. B., Franklin, B. J. (1991). Proceedings of LPSC, v. 21, p 679-693. [22] Barker et al. (2015) Icarus, 273, 346-355 (SLDEM2015 (+LOLA)).

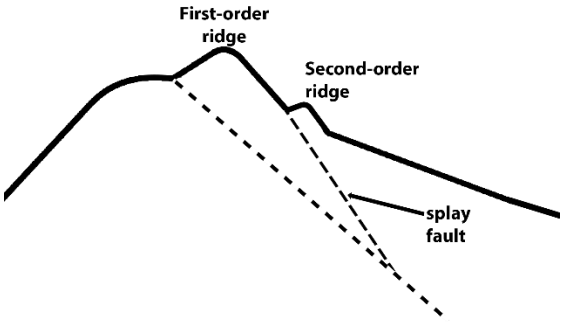

Figure 1. *A cross-section of contractional strain accommodation features from shallow, branching faults. As the stresses increase, the primary fault begins to splay to accommodate the release of stress. At the surface, these branches form second and third-order ridges. Faults do not necessarily break the surface, this is a simplified model. Only ridge faults are shown.*

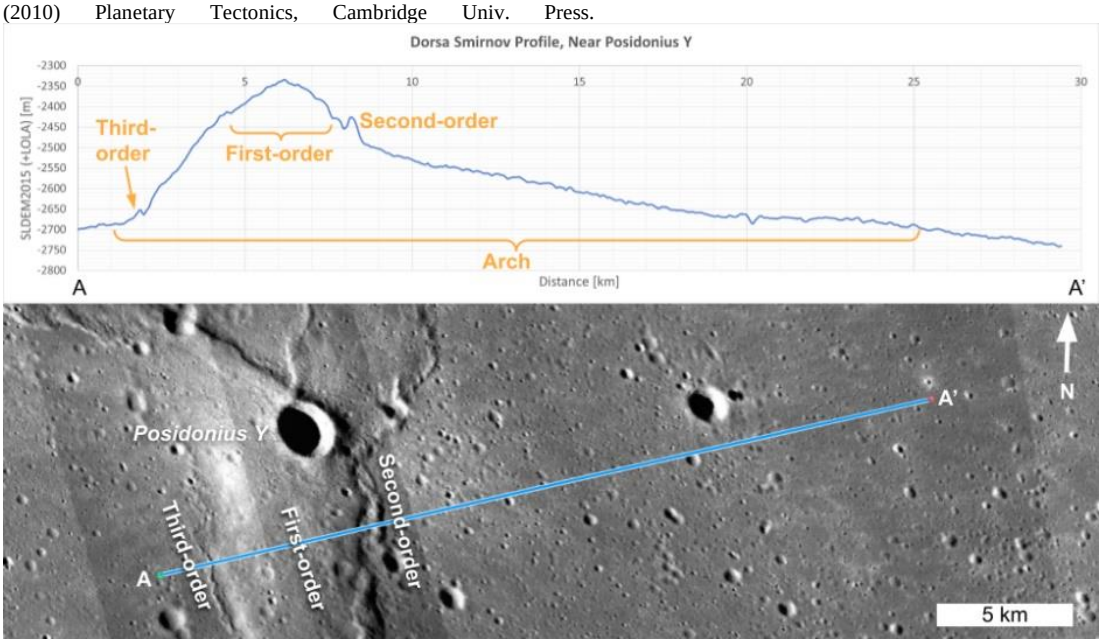

Figure 2. *An example of first, second, and third-order ridges of Dorsa Smirnov in Mare Serenitatis (29.8998 N, 24.8743 E), shown in plan view (base map is the "NACs large inc West" layer in quickmap), and profile view using SLDEM2015 (+LOLA) Lunar Reconnaissance Orbiter elevation data [22]. Note that the arch drawn on the profile is an approximation based on slope steepness in order to provide a sense of scale relative to the different orders of ridges, as well as an example of the visibility of the asymmetry in both profile and NAC views. All ridges here run parallel to the arch, though the WR branches just North of the crater Posidonius Y.*